
Check for updates

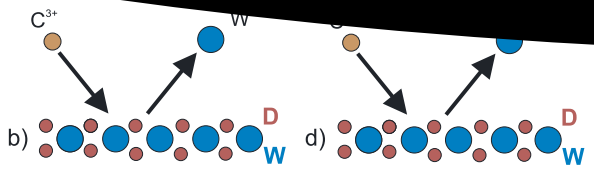

Fig. 1. Scheme of W sputtering processes: a) physical sputtering by fuel ions, b) physical sputtering by impurity ions, c) chemically assisted physical sputtering by fuel ions with release of WD, chemically assisted physical sputtering by impurity ions with release of WD.

operational window, but is not contributing in a prolonged lifetime of the *W* PFCs. Only minimisation of the *W* source with support of the so-called prompt re-deposition effect can help to extend the lifetime of *W* PFCs [13].

Different laboratory studies of *W* bombardment by hydrogen ions have identified the formation of a thin surface layer with high hydrogen content of up to a few percent in the subsurface [14], thus more than four orders of magnitude higher than the solute in *W* for comparable temperatures. The formation is a competition between impinging ion flux, outflux, and diffusion as described in [15,16] and depends in particular on the material temperature. The situation is comparable to beryllium (*Be*) surfaces where molecular dynamics calculations [17] revealed up to 50% *D* in the *Be* surface layer - so-called supersaturation. As consequence an additional mechanism for sputtering can set in: Chemically Assisted Physical Sputtering (*CAPS*). CAPS has been verified by the release of beryllium deuterides, or more precisely by spectroscopic identification and analysis of *BeD* molecules, in PISCES-B and JET [18,19]. The critical questions are if CAPS appears in the case of *W* (Fig. 1c and d) and what is the parameter space of existence? It should be noted, that *CAPS* has not been observed in any fusion-related plasma device in the case of *W* so far, though the worldwide focus in Plasma-Surface Interaction (*PSI*) research is in the qualification of *W* for ITER and DEMO.

In this contribution, we present the first observation [20] and analysis of the *WD* molecule in a fusion-relevant plasma by Optical Emission Spectroscopy (*OES*). Molecular bands of the electronic *WD* transition $^6\Pi \rightarrow ^6\Sigma^+$ were detected close to the *W* PFC surface during the conditions in TEXTOR limiter plasmas. The identification as well as analysis is presented in the Section 2 of the paper.

Additionally, the *WD* transition $^6\Pi \rightarrow ^6\Sigma^+$ has been observed in deuterium high confinement mode (*ELMy H-mode*) discharges in ASDEX Upgrade at the outer target plate made of bulk *W*. Thus, the ASDEX Upgrade experiment gives access to intra-ELM *W* sputtering events by spectroscopic observation of the *WD* molecular bands as well as neutral *W* with the *WI* transition $(5d^5(^6S)6s\,^7S_3 \rightarrow 5d^5(^6S)6p\,^7P_4)$ at $\lambda = 400.9$nm with high temporal and good spatial resolution along the outer target plate in the near Scrape-Off Layer (*SOL*). *CAPS* takes place in both the intra- and inter-ELM phase with impinging ion fluxes consisting of mainly deuterons and an intrinsic impurity mix of *C, B* and *O* ions in the promille range. Details about the experiment including the distribution of the flux ratio of *WD* and *WI* is shown in Section 3.

The summary and conclusion Section 4 provides information on the processes involved in the release of atomic and molecular *W* compounds. The required conditions for the molecular release via *CAPS* are indicated and first conclusions drawn. The potential role of *CAPS* for *W* in the total *W* source as well as the appearance in other experiments like linear devices PSI-2 or MAGNUM-PSI, and larger tokamaks like JET is elaborated.

2. Identification of *WD* molecules in TEXTOR deuterium plasmas

The first spectroscopic identification of the tungsten deuteride molecule was reported by [21] in a deuterium arc discharge close to a tungsten-made injection nozzle with the aid of a Jarrel-Ash monochromator with a resolution of 0.05nm/pix and a photomultiplier as detector. The compressed molecular spectrum between $\lambda = 673$nm and $\lambda = 678$nm was attributed to the $^6\Pi \rightarrow ^6\Sigma^+$ electronic transition of *WD* as indicated in Fig. 2a), whereas it was not clear at the time of the study if the lower state is indeed the electronic ground state. Nevertheless, the rotational P, Q, and R branches were identfied as shown in Fig. 2b) as well as the corresponding spectroscopic molecular constants *B, D,* r_e, and ν provided. Moreover, [21] also observed the corresponding transition of the *WH* molecule at the predicted spectral location confirming that the identification of the tungsten hydride and its isotopomer was

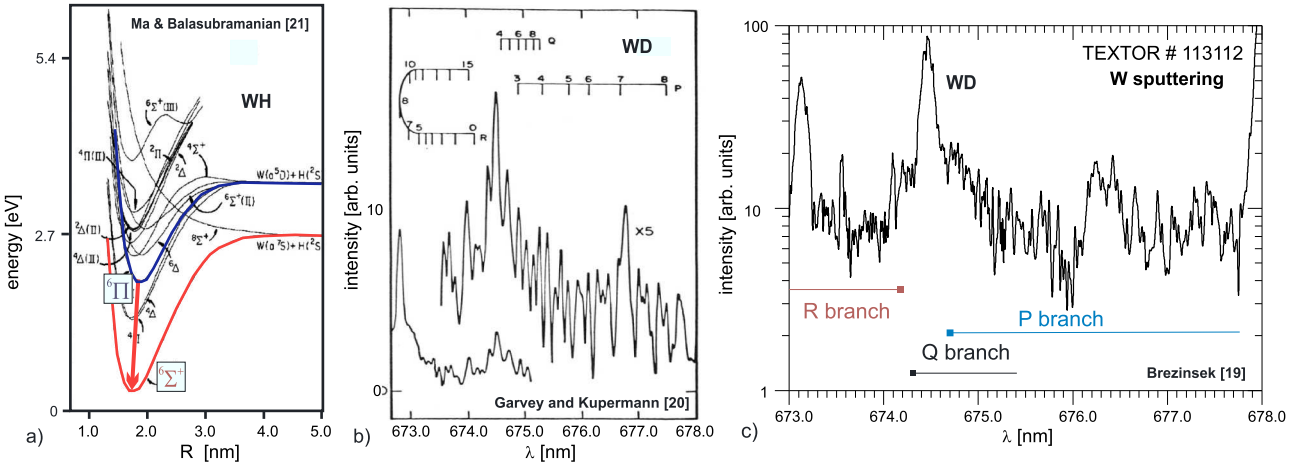

Fig. 2. a) Potential curves of the tungsten hydride (WH) molecule: the electronic transition $^6\Pi \rightarrow ^6\Sigma^+$ is marked according to the identification [22]. b) Reference *WD* $^6\Pi \rightarrow ^6\Sigma^+$ spectrum observed in a low pressure arc discharge close to a tungsten nozzle [21]. C) The corresponding tungsten deuteride *WD* molecular band identified for the first time in a high temperature fusion plasma in front of a W limiter in TEXTOR [20].

of a double prism and [illegible]
with an almost constant resolving power of more than [illegible]
over the full covered wavelength span ($\Delta\lambda_{span}$ of about 364 – 715nm). The system is comparable to [25], but equipped with an one megapixel EMCCD detector by ANDOR which provides higher sensitivity. The price for the simultaneously obtained high resolution spectrum with wide wavelength span is the relative low sensitivity and low temporal resolution of about 200*ms* (frame transfer time of 1*s*) used in the presented measurement. The main spectroscopic features of the *WD* $^6\Pi \rightarrow ^6\Sigma^+$ spectrum can clearly be identified: the line-like shape of the Q-branch at $\lambda = 674.5$nm, the returning R-branch at the lower wavelength end at $\lambda = 673nm$ and the long P-branch tail in the higher range up to $\lambda = 678$nm. Complementary studies with WF_6 injection in a comparable plasma through a stainless steel nozzle, providing a proxy for a neutral *W* gas source and used to determine photon efficiencies [24], have not shown any molecular lines in the corresponding wavelength region. This confirms that the *WD* is not produced within the plasma by recombination, but due to surface reactions at the *W* limiter surface and therefore related to sputtering processes.

The TEXTOR tokamak (closed 12/2013) was a medium-size machine optimised for *PSI* studies with a major radius $R = 1.75$m and a minor radius $a = 0.46$m defined by a toroidal belt limiter made of graphite. Dedicated studies on *W* PFCs were done with the aid of additional limiters installed at variable radial positions in one of two lock systems with optimised diagnostic coverage including image intensified 2*D* CCD cameras with narrowband interference filters and a number of spatially integrating overview spectrometers as described in [7]. However, only the Spectrelle provides simultaneously observation of the standard *WI* line at $\lambda = 400.9$nm and the *WD* band emission range between $\lambda = 673$nm and $\lambda = 678$nm. We revisited previously performed *W* qualification experiments [7] in deuterium at a plasma current of $I_p = 0.35$MA and a toroidal field of $B_t = 2.25T$ in neutral-beam heated discharges with a total input power of $P_{in} = 2.0$MW and a radiated fraction f_{rad} between 0.33 and 0.40. A twin limiter made of graphite and bulk tungsten (*W* from Plansee with 99.97% purity), shown in (Fig. 3a), was positioned 5*mm* behind the last-closed flux surface (Fig. 3b) in the near-SOL and exposed to a number of plasma discharges with four dedicated density phases owing to variation in *D* fuelling. The four phases can be described by the following constant plasma conditions at the radial location of the twin limiter: phase I [$n_e = 0.60 \times 10^{19}$ m^{-3}, $T_e = 84$ eV], phase II [$n_e = 0.85 \times 10^{19}$ m^{-3}, $T_e = 60$ eV], phase III [$n_e = 1.05 \times 10^{19}$ m^{-3}, $T_e = 44$ eV], and phase IV [$n_e = 1.45 \times 10^{19}$ m^{-3}, $T_e = 32$ eV]. The impinging ion flux amounts a few $10^{23} D^+ m^{-2} s^{-1}$ and varies during the density phases as it can be concluded in Fig. 4a) from the Balmer photon fluxes (D_δ and D_γ) from recycling at the limiter. The main impurities were *C* ($c_C \simeq 5.2\%$) and *O* ($c_O \simeq 0.6\%$) which are also responsible for the *W* sputtering as the impinging ion energy of D^+ is below its physical sputtering threshold. Fig. 3b) shows the emission pattern of sputtered *W* in the light *WI* and the deuterium recycling flux in the light of D_α. The sputtering yield of *W* based on *WI* drops in the four phases with decreasing impact energy from 5.2% in phase I, via 2.0% (phase II), and 1.0% (phase III), to finally 0.5% (phase IV) which is consistent with binary-collision approximation calculations with the given impinging impurity mix and ion energy. The limiter temperature was predominantly determined by the active wall heating in TEXTOR to $T_{limiter} \simeq 420$K with minor temperature increase during the plasma discharge by about 80K.

Fig. 4 b) shows the variation of the line-like Q-branch of the *WD* $^6\Pi \rightarrow ^6\Sigma^+$ transition and the standard *WI* transition in the four density

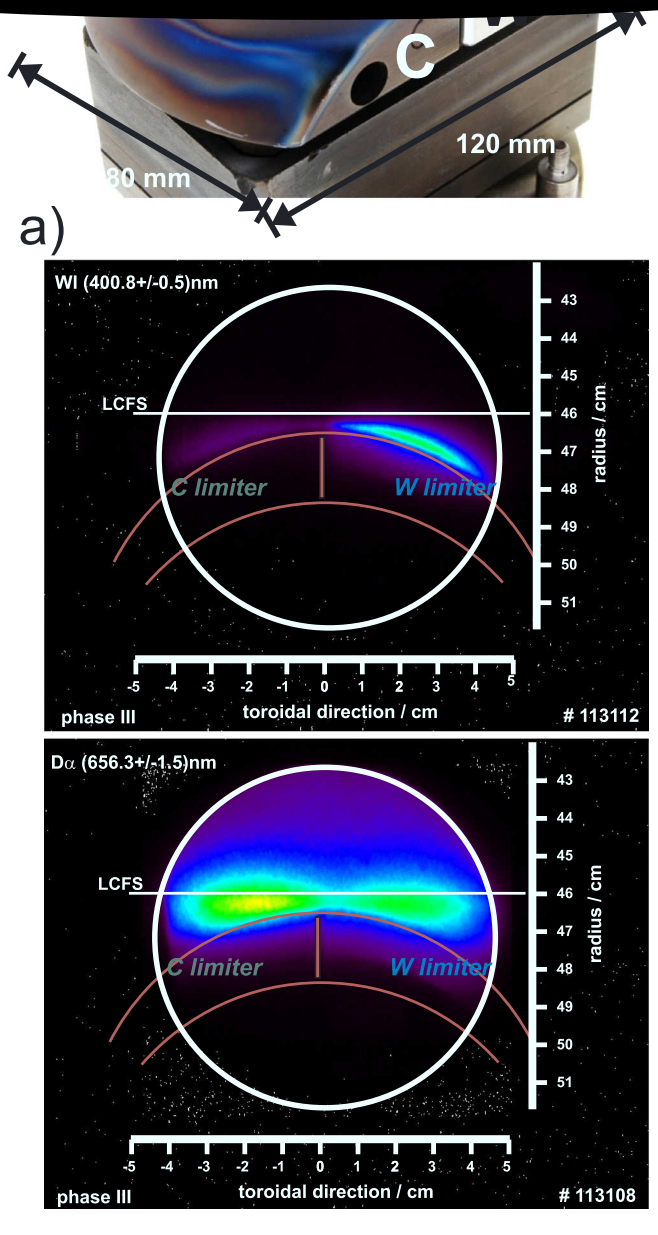

Fig. 3. TEXTOR: a) W/C twin limiter installed in the vacuum lock system after exposition to deuterium plasmas [7]. b) 2D images of interference filtered *WI* ($\lambda = [400.8 + /-0.5]$nm) and D_α ($\lambda = [656.3 + /-1.5]$nm) emission recorded in comparable plasma discharges at $T_e = 44$eV and $n_e = 1.05 \times 10^{19}$m^{-3} at the limiter tip (phase III).

phases described before. The *WI* emission drops monotonically with T_e whereas T_e is a measure for the impact energy via $E_{in} = 3k_B T_e + 2k_B T_i$ and $T_e \simeq T_i$ with the ion temperature T_i. The *WD* emission shows a different behaviour with a peak at the third phase before a drop at lowest T_e occurs. However, in addition to the impact energy, one needs

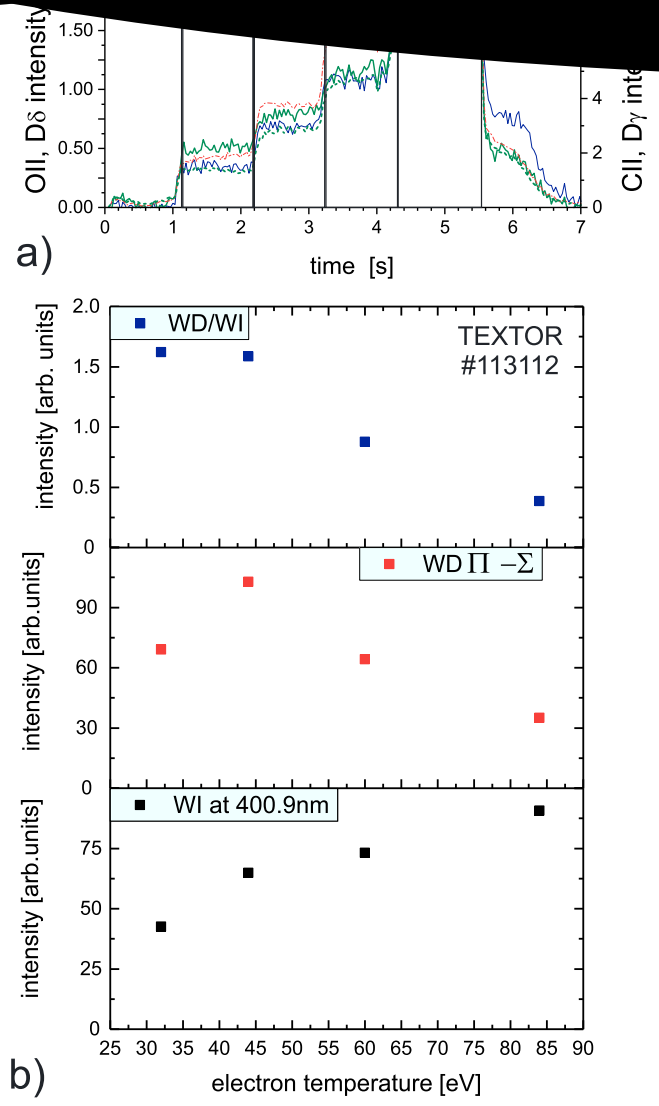

Fig. 4. TEXTOR: a) Variation of the photon fluxes of recycling (D_δ and D_γ), proxy for the impinging ions, and main impurities (*OII* and *CII*) at the W-side of the limiter in the studied discharge scenario with four fuelling steps [7]. b) Variation of *WI* at $\lambda = 400.9$nm and the line-like Q-branch of the ro-vibrational *WD* band ($^6\Pi \rightarrow^6 \Sigma^+$) as function of the local electron temperature established in phases I-IV.

also to consider the ion flux impinging to the limiter which increases almost a factor 4 with the reduction of T_e by a nearly a factor 3 starting from the highest T_e-value in phase I. Ferro and co-workers [26], based on experiments of [14], calculated by a novel global model based on thermodynamics, kinetics, and density functional theory data a continuous increase in the hydrogen content in the near-surface layer of *W* with increasing deuterium flux. The modelled fuel content in *W* rises even steeper, by orders of magnitude, below a critical temperature T_{crit} due to enhanced defect creation and formation of vacancies in *W* with higher hydrogen trapping in it - the so-called supersaturated layer is formed. One can assume that there is a higher probability to release a *WD* molecule at higher impinging ion flux as there is more *D* embedded in this near *W* surface layer at constant temperature. It should be noted, near-surface fuel content in *W*, indicating the chemical sputtering character of CAPS. Further detailed studies at different material or limiter temperatures would have been required to obtain the full matrix or existence diagram of CAPS, but these are due to closure of TEXTOR no longer possible.

3. Identification of *WD* molecules in ASDEX Upgrade deuterium plasmas

Complementary to the first studies in TEXTOR with solely CAPS of *W* caused by impurities, investigations in the *W* divertor of ASDEX Upgrade in deuterium ELMy H-mode discharges have been carried. These H-mode discharges ($B_t = 2.5$T, $I_p = 0.8$MA, $P_{aux} = 7.5$MW) were conducted with the outer-strike line located on a bulk *W* PFC target plate installed in divertor manipulator (DIM II [23]) in the outer leg (Fig. 5b). The corresponding Fig. 5a) shows the *W* target plate (W from Plansee) from the front with the position of the outer strike-line and the spectroscopic observation chords marked. 14 consecutive comparable discharges were executed under attached divertor conditions with an ELM frequency of about $f_{ELM} = 100$Hz permitting the study of CAPS and PS of *W* in the inter and intra-ELM phase caused by impurity ions (B, C, O) and D^+ present in the plasma. Langmuir probes with high temporal resolution were used to determine the local plasma parameters in the inter-ELM phase along the W target plate. The electron temperature and density at the strike-line amounts inter-ELM averaged to $T_{e,SL} = 23$eV and and at the location of the last viewing chord about 8cm away in the near-SOL to $T_{e,SOL} = 15$eV and $n_{e,SOL} = 3 \times 10^{18}\mathrm{m}^{-3}$. The corresponding impinging ion fluxes amount $5 \times 10^{22} D^+\mathrm{m}^{-2}\mathrm{s}^{-1}$ at the strike line and about $1 \times 10^{22} D^+\mathrm{m}^{-2}\mathrm{s}^{-1}$ in the near-SOL. The intra-ELM temperatures and corresponding impact energies are likely one order of magnitude larger. A comparable plasma footprint is also detectable by the infrared thermography providing the surface temperature profile along the *W* target plate: $T_{SL} = 560$K and $T_{SOL} = 410$K which means that the viewing chords on the target plate cover a significant variation of impinging flux, impact energy, and surface temperature conditions.

The plasma and surface conditions in ASDEX Upgrade would fulfill the criteria mentioned before to observe CAPS of *W* at least in the inter-ELM phase as enough deuterium should be retained in the near surface layer. Fig. 6 shows a comparison of emission spectra of a) *WD* $^6\Pi \rightarrow^6 \Sigma^+$ and b) the standard *WI* transition ($5d^5(^6S)6s\,^7S_3 \rightarrow 5d^5(^6S)6p\,^7P_4$) at $\lambda = 400.9$nm recorded in ASDEX Upgrade close to the strike-line and in TEXTOR. The ASDEX Upgrade spectra were recorded in two consecutive discharges with the aid of a high resolution, high throughput spectrometer with narrow wavelength coverage. The ro-vibrational *WD* spectrum in ASDEX Upgrade is very much comparable with the one from TEXTOR with the most characteristic line-like feature of the Q-branch. The ro-vibrational population is comparable in both plasmas though the detailed plasmas parameters are different. The use of the line-like Q-branch as characteristic quantity is therefore verified and can be used to compare it with the *WI* emission at $\lambda = 400.9nm$ as in TEXTOR case. The P-branch seems a bit more pronounced in ASDEX Upgrade and reflects all details shown in [21]. We can conclude that CAPS of *W* takes place in the outer divertor of ASDEX Upgrade - at least under the experimental conditions described before. The poloidal distribution of the *WD* line-like Q branch $^6\Pi \rightarrow^6 \Sigma^+$ radiance, the *WI* radiance of the $5d^5(^6S)6s\,^7S_3 \rightarrow 5d^5(^6S)6p\,^7P_4$ transition, and the ratio of both along the *W* target plate given in the relative target coordinate *s*

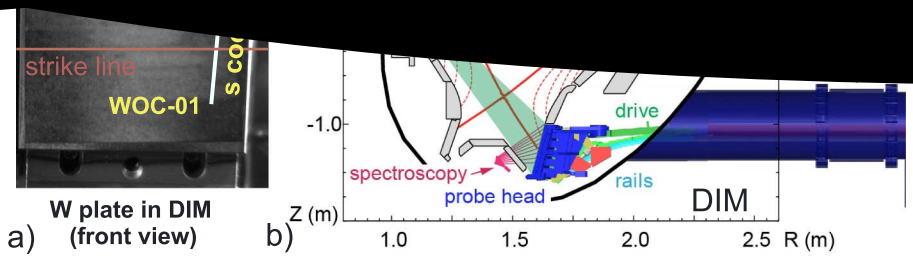

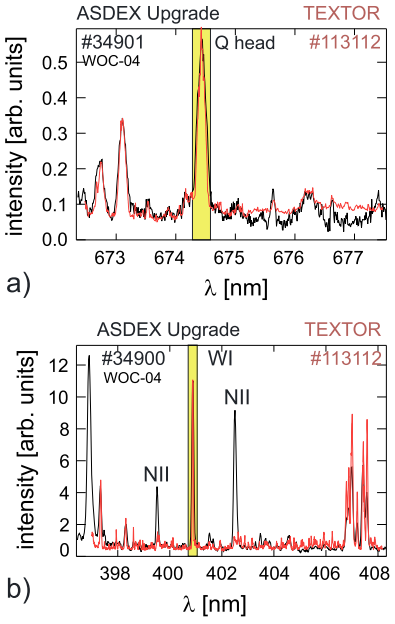

Fig. 6. ASDEX Upgrade and TEXTOR: a) Comparison of the ro-vibrational band emission of *WD* $^6\Pi \rightarrow ^6\Sigma^+$ in the spectral range between 672nm and 678nm with the dominant line-like feature of the Q-branch. b) Comparison of the *WI* line emission ($5d^5(6S)6s^7S_3 -> 5d^5(6S)6p^7P_4$) at $\lambda = 400.9$nm. The TEXTOR spectra are recorded simultaneously in one discharge; the ASDEX Upgrade spectra are recorded in two comparable discharges.

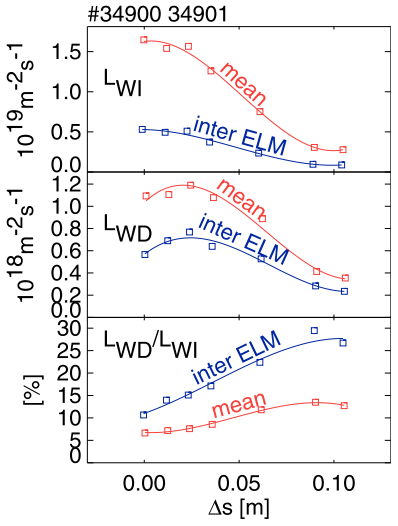

Fig. 7. ASDEX Upgrade: Variation of *WI* radiance at $\lambda = 400.9$nm, the radiance of the line-like Q-branch of the *WD* $^6\Pi \rightarrow ^6\Sigma^+$ band emission, and the ratio of both as function of the relative target coordinate *s*. The averaged inter-ELM distribution as well as the total averaged distribution including all intra- and inter-ELM phases between 3.7s and 7.0s are depicted.

with respect to the outer strike-line position is shown in Fig. 7. The experimental data is recorded in two consecutive self-similar discharges (#34900 and #34901) with appropriate change of the spectrometer wavelength settings. The analysis of OES data is done twofold: a) application of ELM filtering providing the averaged radiance in the inter-ELM phase and exclusion of the high ion impact energy during ELM events and b) total time averaging over the discharge between 3.7s and 7.0s, thus, the mean value of the intra- and inter-ELM phase. The overall profiles of *WD* and *W* radiances for both averaging processes are similar following the impinging ion flux distribution with the maximum emission at the strike-line ($\Delta s = 0$) where also the surface temperature is the highest. However, the ratio of the two radiances reveals a relative increase of *WD* away from the strike-line where the surface temperature is significantly lower permitting a higher deuterium retention in the thin surface layer. In the inter-ELM averaged case are the impact energies still sufficient at this location to erode *W* due to ordinary PS by intrinsic impurities and the impinging deuteron fluxes are still sufficiently high to fill up the vacancies. The spectroscopy suggests that in the near-SOL a higher fraction is released via CAPS than at the strike-line assuming that the *D/XB*-values are comparable in the range of $T_e = 23$eV and $T_e = 15$eV as deduced by ELM filtering from Langmuir Probes.

The intra-ELM *W* phase dominates over the inter-ELM *W* sputtering phase as both, the line-like feature of *WD* $^6\Pi \rightarrow ^6\Sigma^+$ and the *WI* radiance at $5d^5(^6S)6s\,^7S_3 \rightarrow 5d^5(^6S)6p\,^7P_4$ in the mean averaged phase are significantly above the corresponding signals in the inter-ELM phase. This is consistent with previously reported ELM-induced *W* sputtering observations in ASDEX Upgrade done solely with the aid of *WI* emission. Thus, we can first conclude that CAPS is also caused in the intra-ELM phase by impurities as well as energetic impinging deuterons. However, the increase in *WI* is much stronger than in *WD* as indicated by the ratio of the two radiances which can be transferred into the statement that in the presence of high energetic impinging ions the CAPS seems less prominent in comparison to the intra-ELM phase. The probability to release directly a *W* atom is in this case higher than the *WD* molecule by either an impurity ion or a deuteron.

4. Summary and conclusion

We have identified the *WD* $^6\Pi \rightarrow ^6\Sigma^+$ transition in TEXTOR limiter and ASDEX Upgrade divertor plasmas in front of PFCs made of bulk *W*. The ro-vibrational spectra in both plasmas is comparable from the point of view of characteristic features as the line-like Q-branch, the returning R-branch, and the long tail of the P-branch which suggests a

rate coefficients (the
eXcitation rate coefficient X for the observed
the Branching ratio B, are currently unknown. Therefore, we can currently only report on relative changes of the intensities of *WD* as well as relative changes to the best characterised *WI* transition ($5d^5(^6S)6s\,^7S_3 \rightarrow 5d^5(^6S)6p\,^7P_4$) at $\lambda = 400.9$nm. We assume that the ro-vibrational population is unchanged in the plasma parameter range covered which is with $T_e > 10$eV a fully ionising plasma and recombination can in the covered range in TEXTOR and ASDEX Upgrade be excluded.

The destruction of the *WD* molecule can undergo two different paths: a) ionisation of *WD* and formation of the WD^+ molecule by electron impact ionisation and subsequent dissociation into *W* and D^+ or vice versa into W^+ and *D* by electron impact dissociation, and b) dissociation of *WD* by electron impact dissociation into *W* and *D*. Comparable destruction paths have been studied in detail in the case of the *CD* radical with the most probable path via (b) in ionising conditions at lower T_e of below 10eV – like in divertor conditions - and via path (a) at higher temperatures of $T_e > 20$eV - like in limiter conditions. However, there is nor a report on the spectroscopic identification of WD^+ neither any atomic and molecular data exist to verify the paths at this stage, but it is important to state that in both paths a neutral *W* atom during the dissociation can be produced. Thus, it cannot be excluded that *WD* contributes via the potential dissociated product *W* to the line emission of *WI* at e.g. $\lambda = 400.9$nm. This must be taken as caveat when discussing the distribution of *WD* $^6\Pi \rightarrow ^6\Sigma^+$ and *WI* as well as the total *W* sputtering source.

The sputtering of *W* in molecular form as *WD* requires a large fraction of *D* embedded in the top surface of the *W* material matrix. The fuel content in this interaction layer depends on the impinging ion flux and the bulk temperature which determines the formation of vacancies by ion damage. This process competes with desorption and outflux of *D* as well as with diffusion of *D* deeper into the matrix. Recent experimental observations [14] and novel modelling [26] showed the formation of a narrow supersaturation layer in *W* with high *D* content in the percent range below a critical surface temperature T_{crit} which would provide most favourable conditions for chemically assisted physical sputtering CAPS of *W*. The fuel content in the narrow surface layer rises in general with increase of the impinging deuteron flux, roughly one order in retention per one order of flux, and decrease with the material temperature. The ion flux conditions in TEXTOR and ASDEX Upgrade are in the range of $0.1 - 2.0 \times 10^{23}\mathrm{Ds^{-1}m^{-2}}$ which corresponds to $T_{crit} \simeq 550$K and a supersaturated layer below this temperature. The third parameter required for CAPS is the energy of the impinging projectiles which must overcome a characteristic binding energy. The variation in the observed intensity of *WD* in TEXTOR and ASDEX Upgrade can be attributed to changes in these three parameters which is in contrast to the temperature independent ordinary physical PS. In TEXTOR impurity ions are solely responsible for the release whereas in ASDEX Upgrade also fast deuterons during ELM events contribute on top of the impurity ions to CAPS. Therefore, we can conclude, that the release mechanism is via cascades followed by a release and not via a capture of a loosely bound *W* at the surface by an impinging deuteron. However, it is unknown what the minimum impact energy is to cause the process and dedicated experiments seem required to determine it. Most relevant is the determination of the threshold in the relevant impinging ion flux range in the order of about $10^{22} - 10^{24}\mathrm{Ds^{-1}m^{-2}}$ present in divertor conditions in fusion devices which limits the number of relevant test devices to high flux experiments like the linear plasma devices PSI-2 and MAGNUM-PSI. Certainly, the inertially cooled bulk W course the penetration depth of the potentially resulting *W* atom from the *WD* dissociation will be slightly larger due to the two step process than of the bare physically sputtered *W* atom. Thus, if ionisation takes place via destruction channel (a) or (b), a large fraction will return to the surface within one Larmor radius at the high magnetic fields above $B_t > 2T$ present in TEXTOR and ASDEX Upgrade. Therefore, the contribution of *WD* to the net *W* erosion source above the threshold energies for bare PS is even smaller than to the gross erosion source determined by OES. Nevertheless, further experiments with variation of all three parameters: impinging ion flux, impact energy, and surface temperature are required to quantify the exact contributions. In particular, the threshold energy for the CAPS process might below the one for bare PS as the binding energy might be reduced. This would permit a potential *W* erosion source at low impact energies where *W* erosion is usually assumed to be switched off. Potentially, easier re-erosion and transport of *W* towards remote areas might follow as observed e.g. in JET in the louvre area of the divertor. Dedicated experiments in JET and ASDEX Upgrade are currently foreseen to investigate this potential way of *enhanced W* material transport via CAPS. Better understanding in this topic is required in order to improve the *W* erosion and transport modelling in the divertor in view of ITER and DEMO *W* PFC life time predictions.

Declaration of interests

The authors declare that they have no known competing financial interests or personal relationships that could have appeared to influence the work reported in this paper.

Supplementary material

Supplementary material associated with this article can be found, in the online version, at 10.1016/j.nme.2018.12.004

References

[1] R. Neu, et al., Phys. Plasmas 20 (2013) 056111.
[2] A. Pospieszczyk, et al., J. Nucl. Mater. 290-3 (2001) 947.
[3] G.F. Matthews, et al., Phys. Scr. T145 (2011) 014001.
[4] S. Brezinsek, et al., J. Nucl. Mater. 463 (2015) 11.
[5] R.A. Pitts, et al., This conference.
[6] T. Pütterich, et al., Plasma Phys. Control. Fusion 55 (2013) 124036.
[7] S. Brezinsek, et al., Phys. Scr. T145 (2011) 14016.
[8] C. Guillemaut, et al., Plasma Phys. Control. Fusion 57 (2015) 085006.
[9] R. Dux, et al., J. Nucl. Mater. 390-1 (2009) 858.
[10] T. Abrams, et al., Nucl. Fusion 57 (2017) 056034.
[11] G. van Rooij, et al., J. Nucl. Mater. 438 (2013) S42.
[12] R. Dux, et al., Nucl. Mater. Energy 12 (2017) 28.
[13] A. Kirschner, et al., Plasma Phys. Control. Fusion 60 (2018) 014041.
[14] L. Gao, et al., Nucl. Fusion 57 (2017) 016026.
[15] E. Hodille, et al., Phys. Scr. T167 (2017) 014011.
[16] K. Heinola, et al.,. This conference.
[17] C. Björkas, et al., New J. Phys. 11 (2009) 123017.
[18] D. Nishijima, et al., Plasma Phys. Control. Fusion 50 (2009) 125007.
[19] S. Brezinsek, et al., Nucl. Fusion 54 (2014) 103001.
[20] S. Brezinsek, et al., Presented at the International Conference of Fusion Reactor Materials, Aachen, 2015.
[21] J.F. Garvey, A. Kupermann, J. Phys. Chem. 9 (1986) 4583.
[22] Zhongxin Ma, K. Balasubramanian, Chem. Phys. Lett. 181 (1991) 467.
[23] A. Herrmann, et al., Fusion Eng. Des. 98–99 (2015) 1496.
[24] S. Brezinsek, et al., Phys. Scr. T170 (2017) 014052.
[25] S. Brezinsek, et al., Plasma Fusion Res. 3 (2008) S1041.
[26] E. Hodille, et al., Phys. Rev. Mater. (2018). Accepted for publication